Supplementary Information for:

Giant elastic-wave asymmetry in a linear passive circulator

Yabin Hu[1, 2], Yongbo Li[1], Yongquan Liu[3, *], Bing Li[1, *], Johan Christensen[2, *]

[1] *School of Aeronautics, Northwestern Polytechnical University, Xi'an, Shaanxi, 710072, China*

[2] *IMDEA Materials Institute, Calle Eric Kandel, 2, 28906 Getafe, Madrid, Spain*

[3] *State Key Laboratory for Strength and Vibration of Mechanical Structure, School of Aerospace Engineering, Xi'an Jiaotong University, Xi'an, 710049, China*

**Corresponding authors:* liuy2018@xjtu.edu.cn; bingli@nwpu.edu.cn; johan.christensen@imdea.org

This Supplementary Information includes:

1. The dispersion relation of flexural-mode for the unit cell in circulator

We designed the unit cell to tailor the wave vector, which is realized by arranging varying-length cantilever beams on the both sides of waveguide channel. The detailed size of unit cell is shown in Fig. S1(a). Here, $H = 10\,mm$, $h = 5\,mm$, $\delta = 10\,mm$, s is the length of cantilever beams, which determines the dispersion profile. We take the unit cell with $s = 8\,mm$ as an example to derive the dispersion. The whole region is divided into two parts. Part I is the waveguide channel and part II are the cantilever beams. The out-of-plane displacement in part I can be written as

$$w1 = \Phi(y) \cdot e^{i(\omega t - k_x x)} \tag{S1}$$

where, ω is the angular frequency and k_x is the wave vector in x direction. Using the classical Kirchhoff plate theory, we substitute Eq. (S1) into the flexural wave equation and get

$$\Phi^{(4)}(y) - 2{k_x}^2\Phi^{(2)}(y) - \left(k^4 - {k_x}^4\right)\Phi(y) = 0 \tag{S2}$$

The solution of Eq. (S2) can be written as

$$\Phi(y) = C_1 e^{\sqrt{-k^2+{k_x}^2}y} + C_2 e^{-\sqrt{-k^2+{k_x}^2}y} + C_3 e^{\sqrt{k^2+{k_x}^2}y} + C_4 e^{-\sqrt{k^2+{k_x}^2}y} \tag{S3}$$

In the equation, if $k > k_x$, we let $\xi_1 = \sqrt{k^2 - {k_x}^2}$ and $\xi_2 = \sqrt{k^2 + {k_x}^2}$. Conversely, if $k < k_x$, $\xi_1 = \sqrt{{k_x}^2 - k^2}$ and $\xi_2 = \sqrt{k^2 + {k_x}^2}$. C_1, C_2, C_3, C_4 are undetermined coefficients. Ignoring time harmonic term $e^{i\omega t}$, the displacement $w1$ in the waveguide can be written in the following two forms,

$$k_x > k: \begin{cases} w1 = \left(Acosh(\xi_1 y) + Bcosh(\xi_2 y)\right)e^{-ik_x x} \\ \xi_1 = \sqrt{{k_x}^2 - k^2},\ \xi_2 = \sqrt{{k_x}^2 + k^2} \end{cases} \tag{S4}$$

$$k_x < k: \begin{cases} w1 = \left(Acos(\xi_1 y) + Bcosh(\xi_2 y)\right)e^{-jk_x x} \\ \xi_1 = \sqrt{k^2 - {k_x}^2},\ \xi_2 = \sqrt{k^2 + {k_x}^2} \end{cases} \tag{S5}$$

A and B are two undetermined coefficients. As the width h of cantilever beams is much smaller than the wavelength, the displacement w_{II} in part II can be written in the form of plane wave,

$$w_2 = a\, e^{-iky} + be^{iky} + ce^{-ky} + de^{ky} \tag{S6}$$

Applying the continuous condition for displacement, slope, bending moment and shear force at the interface between part I and part II ($y = \frac{\delta}{2}$), then we get

$$\int_{-H/2}^{H/2} w1\, dx = \int_{-w/2}^{w/2} w2\, dx \tag{S7}$$

$$\int_{-H/2}^{H/2} \frac{\partial w1}{\partial y} dx = \int_{-w/2}^{w/2} \frac{\partial w2}{\partial y} dx \tag{S8}$$

$$\int_{-H/2}^{H/2} \frac{\partial^2 w1}{\partial y^2} + \nu \frac{\partial^2 w1}{\partial x^2} dx = \int_{-w/2}^{w/2} \frac{\partial^2 w2}{\partial y^2} + \nu \frac{\partial^2 w2}{\partial x^2} dx \tag{S9}$$

$$\int_{-H/2}^{H/2} \frac{\partial}{\partial y} \left(\frac{\partial^2 w1}{\partial y^2} + \nu \frac{\partial^2 w1}{\partial x^2}\right) dx = \int_{-w/2}^{w/2} \frac{\partial}{\partial y} \left(\frac{\partial^2 w2}{\partial y^2} + \nu \frac{\partial^2 w2}{\partial x^2}\right) dx \tag{S10}$$

For the free boundary at the end of cantilever beams ($y = \frac{\delta}{2} + s$), the bending moment and shear force equal zero, then we can get

$$\int_{-w/2}^{w/2} \frac{\partial^2 w1}{\partial y^2} + \nu \frac{\partial^2 w1}{\partial x^2} dx = 0 \tag{S11}$$

$$\int_{-w/2}^{w/2} \frac{\partial}{\partial y} \left(\frac{\partial^2 w1}{\partial y^2} + \nu \frac{\partial^2 w1}{\partial x^2}\right) dx = 0 \tag{S12}$$

Combining Eq. (S7) ~ Eq. (S12), we can build the relation between matrix T and the coefficient vector $[A\ B\ a\ b\ c\ d]^T$,

$$\boldsymbol{T} \cdot [A\ B\ a\ b\ c\ d]^T = \boldsymbol{0} \tag{S13}$$

$$\boldsymbol{T} = \begin{bmatrix} T_{11} & T_{12} & -he^{-ik\frac{\delta}{2}} & -he^{ik\frac{\delta}{2}} & -he^{-k\frac{\delta}{2}} & -he^{k\frac{\delta}{2}} \\ T_{21} & T_{22} & ikhe^{-ik\frac{\delta}{2}} & -ikhe^{ik\frac{\delta}{2}} & khe^{-k\frac{\delta}{2}} & -khe^{k\frac{\delta}{2}} \\ T_{31} & T_{32} & -k^2he^{-ik\frac{\delta}{2}} & -k^2he^{ik\frac{\delta}{2}} & k^2he^{-k\frac{\delta}{2}} & k^2he^{k\frac{\delta}{2}} \\ T_{41} & T_{42} & -ik^3he^{-ik\frac{\delta}{2}} & ik^3he^{ik\frac{\delta}{2}} & k^3he^{-k\frac{\delta}{2}} & -k^3he^{k\frac{\delta}{2}} \\ 0 & 0 & e^{-ik(\frac{\delta}{2}+s)} & e^{ik(\frac{\delta}{2}+s)} & -e^{-k(\frac{\delta}{2}+s)} & -e^{k(\frac{\delta}{2}+s)} \\ 0 & 0 & ie^{-ik(\frac{\delta}{2}+s)} & -ie^{ik(\frac{\delta}{2}+s)} & -e^{-k(\frac{\delta}{2}+s)} & e^{k(\frac{\delta}{2}+s)} \end{bmatrix} \tag{S14}$$

$T_{11} = \frac{2cos\,(\frac{\delta}{2}\xi_1)sin\,(\frac{Hk_x}{2})}{k_x}$, $T_{12} = \frac{2cosh\,(\frac{\delta}{2}\xi_2)sin\,(\frac{Hk_x}{2})}{k_x}$,

$T_{21} = \frac{-2sin\,(\frac{\delta}{2}\xi_1)sin\,(\frac{Hk_x}{2})\xi_1}{k_x}$, $T_{22} = \frac{2sinh\,(\frac{\delta}{2}\xi_2)sin\,(\frac{Hk_x}{2})\xi_2}{k_x}$,

$T_{31} = \frac{2cos\,(\frac{\delta}{2}\xi_1)(k_x{}^2 \upsilon + \xi_1{}^2) sin\,(\frac{Hk_x}{2})}{k_x}$, $T_{32} = \frac{2cosh\,(\frac{\delta}{2}\xi_2)(k_x{}^2 \upsilon - \xi_2{}^2) sin\,(\frac{Hk_x}{2})}{k_x}$,

$T_{41} = \frac{2sin\,(\frac{\delta}{2}\xi_1)\xi_1(k_x{}^2(2-\upsilon) + \xi_1{}^2) sin\,(\frac{Hk_x}{2})}{k_x}$, $T_{42} = \frac{2sin\,h\left(\frac{\delta}{2}\xi_2\right)\xi_2(-k_x{}^2(2-\upsilon) + \xi_2{}^2) sin\,(\frac{Hk_x}{2})}{k_x}$,

Only when $\det \boldsymbol{T} = 0$ is satisfied, the coefficient $[A\ B\ a\ b\ c\ d]^T$ is the nonzero vector. In the case, we can calculate the wave vector k_x at different frequencies and plot the dispersion relation of two flexural modes, which is shown in Fig. S1(b).

2. The impedance characteristics of unit cells

Here we derived the impedance of flexural modes based on homogenized model. As shown in Fig. S2(a), asymmetric behavior can also be realized in the elastic waveguide system which consists of homogenized unit cells. The unit cell is enlarged in the dashed box. It contains two isotropic materials with different Young's modulus. The waveguide channel has the constant modulus E_0, while the boundary modulus E_i varies along the waveguide. The modulus profile E_i is exhibited in Fig. S2(b) and the corresponding refraction index n_i increases linearly. The relation between E_i and n_i can be expressed by

$$E_i = \frac{E_0}{n_i{}^4} \qquad \text{(S15)}$$

According to Eq. (S15), the Young's modulus E_i alters along the waveguide, as shown in Fig. S2(b). In this case, flexural waves excited at the left port will propagate along the $+x$ direction. On the contrary, they will be blocked and reflected back if excited at the right port. The simulated out-of-plane displacement fields at 4.5 kHz are shown in Fig. S2(a).

The underlying physical mechanism can also be explained by dispersion relation of two flexural modes. We select five unit cells to investigate the evolution of wave vector k_x, as shown in Fig. S2(c). Mode 1 (blue dots) excited at the left port can always intersect with the frequency 4.5 kHz (the black dashed line), which means flexural waves in mode 1 are supported in the waveguide. Although the intersection points are invisible at $x = 80\,mm$ and $x = 100\,mm$, they still exist because the grating constant H can be small enough to ensure the branch of mode 1 can coincide with 4.5 kHz at far location. From the opposite direction, the intersection points between mode 2 and 4.5 kHz can be observed until the cut-off position of $x = 60\,mm$, which determines mode 2 will not supported beyond this location. The yellow solid line represents the wavenumber k of flexural waves in infinite plate. Below the yellow solid line, flexural waves will converge to the boundary and be converted into surface waves. In the end, the asymmetric waveguide based on homogenized unit cells are also be explained by the evolution of wave vector k_x, which is in the same as the waveguide based on cantilever beam model in the main text.

Based on the above analysis, we confirm that the homogeneous waveguide exhibits same physical property as discrete waveguide in the main text, which allow us to calculate the impedance of flexural waves by the homogenized unit cells. We select the unit cell at $x = 70\,mm$ with $E_0 = 200\,GPa$ and $E_i = 959\,MPa$, which supports two flexural modes at 4.5 kHz. The unit cell is shown in Fig. S3(a), whose geometric parameters are $\delta = 20\,mm, l = 5\,mm, H = 10\,mm.$ For mode 1, $k_x > k_0$ and the displacement $w1$ is expressed in Eq. (S4). For mode 2, $k_x < k_0$ and the displacement $w1$ is expressed in Eq. (S5). The dispersion relations of two flexural modes are provided in Fig. S3(b).

The out-of-plane displacement w in the middle and boundary of waveguide channel is denoted as,

$$mode\ 1\text{:}\ \begin{cases} w_{y=0} = A + B \\ w_{y=\delta/2} = Acosh(\xi_1\delta/2) + Bcosh(\xi_2\delta/2) \end{cases} \tag{S16}$$

$$mode\ 2\text{:}\ \begin{cases} w_{y=0} = A + B \\ w_{y=\delta/2} = Acos(\xi_1\delta/2) + Bcosh(\xi_2\delta/2) \end{cases} \tag{S17}$$

We extract the average displacement at $y = 0$ and $y = \delta/2$ based on the simulated eigenmodes in Fig. S3(c) and (d). By substituting $w_{y=0}$ and $w_{y=\delta/2}$ into Eq. (S16) and Eq. (S17), the coefficients A and B can be solved. The distribution of displacement w and two constituting terms are plotted in Fig. S3(c) and (d). The first term $Acosh(\xi_1 y)$ and $Acos(\xi_1 y)$ are much more than the second term $Bcosh(\xi_2 y)$ and $Bcos(\xi_2 y)$ for mode 1 and mode 2, respectively. Therefore, the out-of-plane displacement w for mode 1 and mode 2 are approximately equal to

$$k_x > k\text{:}\ \begin{cases} w = Acosh(\xi_1 y)e^{-ik_x x} \\ \xi_1 = \sqrt{{k_x}^2 - k^2},\ \xi_2 = \sqrt{{k_x}^2 + k^2} \end{cases} \tag{S18}$$

$$k_x < k: \begin{cases} w = Acos(\xi_1 y)e^{-ik_x x} \\ \xi_1 = \sqrt{k^2 - {k_x}^2},\ \xi_2 = \sqrt{k^2 + {k_x}^2} \end{cases} \tag{S19}$$

The impedance Z of flexural waves can be defined by $Z = \frac{M_x}{\varphi}$. M_x and φ_x are bending moment and slope in x direction, which can be expressed by $-D(\partial_{xx}w + \upsilon\partial_{yy}w)$ and $\partial_x w$, respectively. $D = \frac{E\tau^3}{12(1-\nu^2)}$ is the bending stiffness of plate and υ is the Poisson rate. Applying Eq. (S18) and Eq. (S19) into

the expression of impedance Z. Eventually, the impedance Z has the following unified form,

$$Z = iD(\frac{k^2\nu}{k_x} + k_x(1-\nu)) \tag{S20}$$

According to Eq. (S20), the impedance Z only depends on wave vector k_x if the medium in waveguide channel keeps constant. Therefore, we can tailor the impedance of waveguide by assigning different unit cells. Although the conclusion is deduced based on homogeneous effective medium, it is still available to unit cell based on cantilever beam in the following sections.

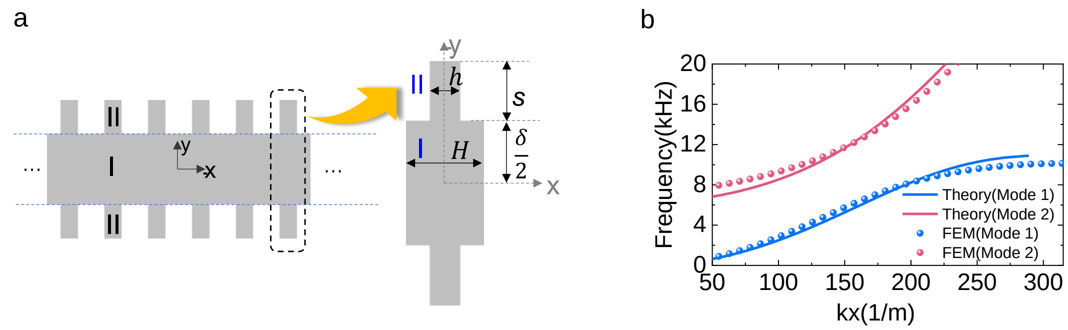

Fig. S1 The dispersion relation of unit cell in circulator. (a) The basic parameters of unit cell. **(b)** The analytical and simulated dispersion relations for mode 1 and mode 2.

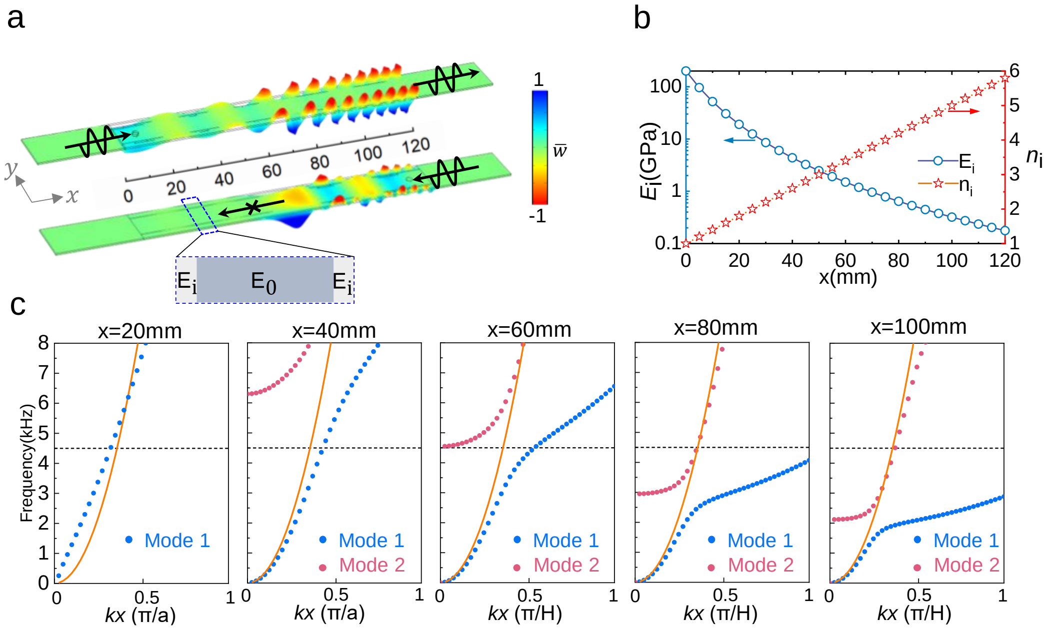

Fig. S2 Asymmetric transmission of elastic waves by homogeneous waveguide. (a) The simulated out-of-plane displacement fields at 4.5 kHz. The unit cell is enlarged in the inset. **(b)** The elastic modulus E_i of waveguide boundary and corresponding refraction index n_i along the waveguide. **(c)** The dispersion relations of two flexural modes for five unit cells. The yellow solid line represents the wavenumber of plate.

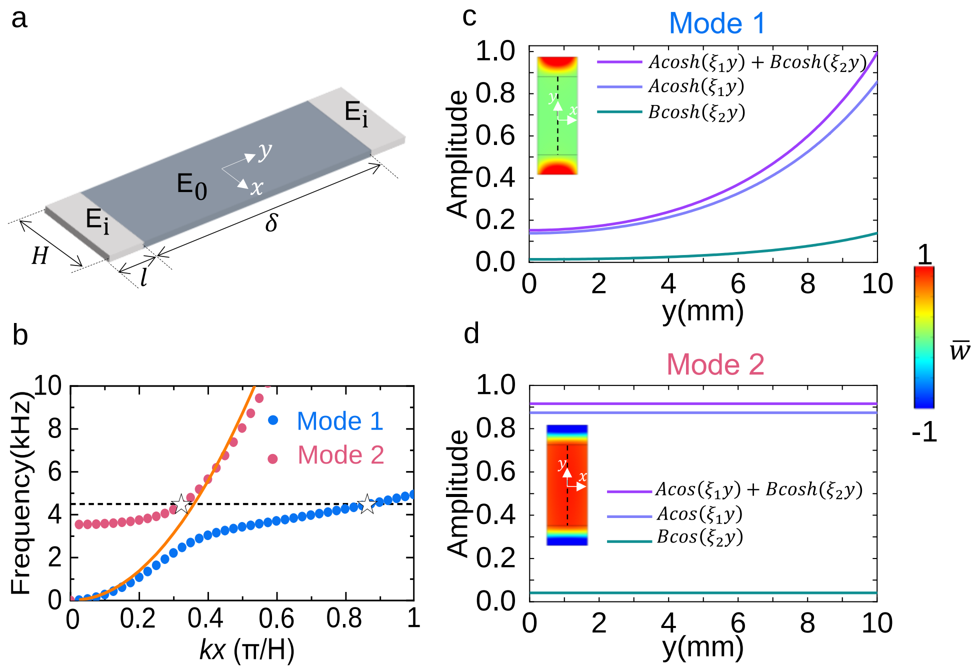

Fig. S3 The analysis of flexural-wave impedance in the waveguide. (a) The schematic of unit cell. **(b)** The dispersion relation of unit cell. Two flexural modes at 4.5 kHz are marked by stars. The eigenmodes for mode 1 and mode 2 are shown in **(c)** and **(d)**, respectively.

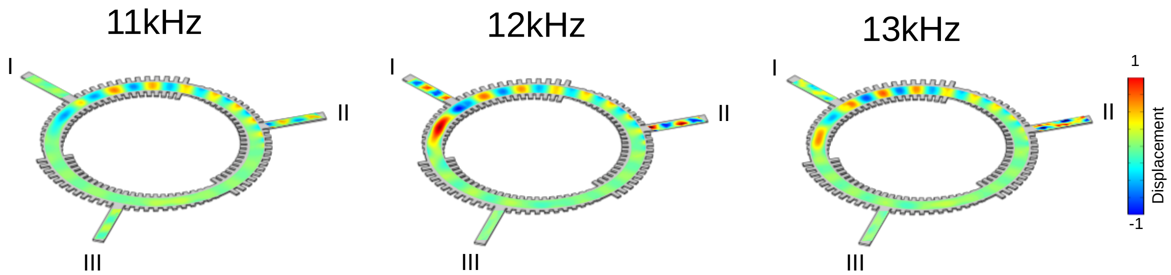

Fig. S4 The experiment results at other frequencies

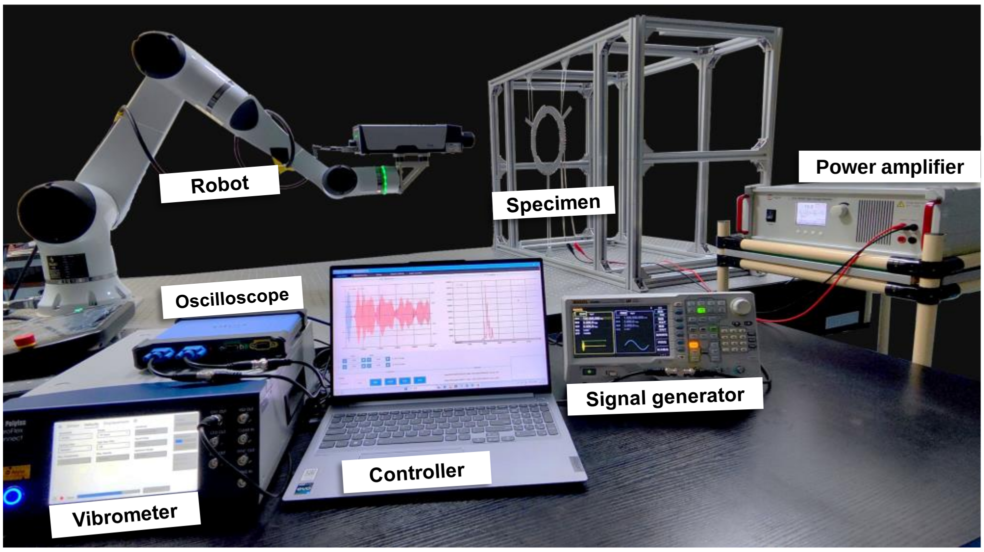

Fig. S5 The experiment setup

Supplementary table S1. The detail sizes of cantilever beams in unit cells of circulator

azimuth (°)	lengths of cantilever beam (mm)	azimuth (°)	lengths of cantilever beam (mm)
0	6.70	62.4	1.03
4.8	6.88	67.2	1.77
9.6	7.05	72	2.78
14.4	7.22	76.8	3.59
19.2	7.39	81.6	4.10
24	7.58	86.4	4.36
28.8	7.84	91.2	4.38
33.6	8.12	96	4.86
38.4	8.44	100.8	5.13
43.2	8.95	105.6	5.50
48	9.47	110.4	5.87
52.8	10.00	115.2	6.30
57.6	0.00	120	6.70